

Most Probable Transitions from Metastable to Oscillatory Regimes in a Carbon Cycle System

Wei Wei^{1,†}, Jianyu Hu^{1,*}, Jianyu Chen^{1,‡} and Jinqiao Duan^{2,§}

¹Center for Mathematical Sciences, Huazhong University of Science and Technology,
Wuhan, Hubei 430074, China.

²Departments of Applied Mathematics & Physics, Illinois Institute of Technology, Chicago, IL 60616, USA.

Abstract

Global climate changes are related to the ocean's store of carbon. We study a carbonate system of the upper ocean, which has metastable and oscillatory regimes, under small random fluctuations. We calculate the most probable transition path via a geometric minimum action method in the context of the large deviations theory. By examining the most probable transition paths from metastable to oscillatory regimes for various external carbon input rates, we find two different transition patterns, which gives us an early warning sign for the dramatic change in the carbonate state of the ocean.

Keywords: Large deviation principle, geometric minimum action method, the most probable transition path, carbon cycle, early warning.

Lead paragraph:

Human activities have been producing more and more carbon dioxide into the carbon cycle, which in turn, significantly influence the climate nowadays. We investigate an oceanic carbonate system that plays a major role in the global carbon cycle. This system has metastable and oscillatory regimes. Due to the small random fluctuations to the external carbon input rate, this system undergoes a transition between these two regimes. We use a geometric minimum action method to capture this transition phenomenon and compute the most probable transition path. We uncover that as the external CO_2 input rate ν changes, two different transition patterns occur with $\nu \approx 0.2$ as a critical value: (i) At a lower level external CO_2 input rate (lower than 20%), the concentration of CO_3^{2-} undergoes a larger excursion to shift to the oscillatory state. (ii) But at a higher

[†]Email: weiw16@hust.edu.cn

^{*}Email: jianyuhu@hust.edu.cn

[‡]Email: jianyuchen@hust.edu.cn

[§]Email: duan@iit.edu

^{*}is the corresponding author

level external CO_2 input rate (larger than 20%), a much smaller excursion of the concentration of CO_3^{2-} leads to a transition to the oscillatory state. Moreover, as the external CO_2 input rate ν increases, the arrival value of the concentration of CO_3^{2-} decreases from over $150 \mu\text{mol} \cdot \text{kg}^{-1}$ to around $50 \mu\text{mol} \cdot \text{kg}^{-1}$.

1 Introduction

The carbon cycle is the biogeochemical cycle in which photosynthesis converts carbon dioxide (CO_2) to organic carbon and respiration converts organic carbon back to CO_2 . Human activities are adding more and more carbon into the atmosphere and become an important part of the carbon cycle. Recently, due to global warming, extreme weather has become more and more common. As a main part of Earth's carbon cycle, the oceanic carbonate system worths our attention.

Rothman [17] introduced a model to describe the dynamical behaviors of the carbonate system of the upper ocean. He took human activities and volcanic emissions as an external source of carbon dioxide (CO_2). Using the model, he demonstrated that as the external CO_2 inputs increases, both the dissolved inorganic carbon w and carbonate ions CO_3^{2-} near a stable state may be disrupted or excited to be near a higher oscillatory level, and eventually come back to the stable state. These large amplitude oscillations are often associated to climate change and mass extinctions. However, Rothman did not take random fluctuations in the strength of the external source of CO_2 . But due to unexpected events and measurement error, it is reasonable to take such fluctuations into consideration.

We look into the same model as Rothman, but include inevitable random fluctuations to the external carbon input. We are interested in the bistable case of this model. Because in original Rothman's model, if the system starts near the stable state, it will never reach the oscillatory state. But in the presence of fluctuations, no matter how small it may be, in a long run, this system will stop staying at the original stable state and travel to an oscillatory state [4, 16]. These fluctuations make the Rothman's deterministic model a stochastic dynamical system.

Stochastic dynamical systems are mathematical models for complex phenomena in physical, chemical and biological sciences [1, 5, 6, 7]. A stochastic system may possess multistable regimes, such as one stable state and one stable limit cycle (the oscillatory state), with a sandwiched unstable limit cycle. There are many literature concerning the first passage time of transition from the stable fixed point to the limited cycle [8, 9, 10, 11, 18]. The transition behaviors are also related to early warning signs [13, 14]. We study the transitions between stable regimes under random fluctuations [2, 3, 12]. Large deviations theory is a useful tool that can be used to capture transition behaviors of stochastic dynamical system. Roughly speaking, large deviations theory measures how small the probability of rare events is. It generalized the concept of potential of the gradient system to quasi-potential of the non-gradient system, which is a minimizer of the action of paths connecting two ends. We regard such a minimizer as our most probable transition path that connects the metastable state and oscillatory state. We use the geometric minimum action method, which was proposed by M. Heymann and E. Vanden-Eijnden [15], to find the minimizer. It used a reparametrization method to transfer infinity time scale to finite time scale and then numerically solved

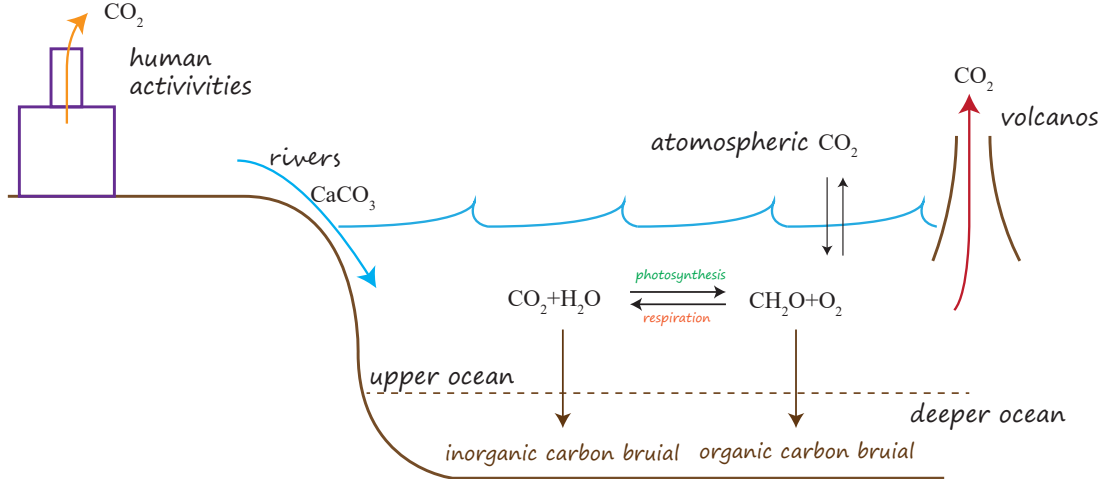


Figure 1: An oceanic carbonate system

an Euler-Lagrange equation to obtain the minimizer.

We will look into the bistable case of the stochastic carbonate system. We will use the geometric minimum action method to find the most probable transition path for different external CO₂ input rate. Based on the numerical simulations, we uncover two different transition patterns.

This paper is arranged as follows. In section 2, we will briefly introduce the carbon cycle model. The theoretical background of the geometric minimum action method will be provided in section 3 and in section 4, we will show our numerical experiments and explanation.

2 An oceanic carbonate system

In the marine carbon cycle, we look into the evolution of the carbonate system in the upper ocean, which is illustrated in Figure 1. We consider a well mixed open system and investigate the carbonate ions in the form of CO_3^{2-} , HCO_3^- and CO_2 . A main carbonate input is the dissolved CaCO_3 carried in by rivers. Respiration is a main source of CO_2 . Volcanic emissions, human activities are regarded as an external source of CO_2 . The precipitation and transportation to lower ocean of CaCO_3 is a main carbonate output of the system. Photosynthesis is a main export of CO_2 of the system.

Rothman [17] introduced a model to describe dynamical behaviors of the carbonate system and it is formulated as follows.

$$dc = [\mu [1 - bs(c, c_p) - \theta \bar{s}(c, c_x) - \nu] + w - w_0] f(c) dt, \quad (2.1)$$

$$dw = [\mu [1 - bs(c, c_p) + \theta \bar{s}(c, c_x) + \nu] - w + w_0] dt. \quad (2.2)$$

Here, w denotes the total dissolved inorganic carbon, that is

$$w = [\text{CO}_2] + [\text{HCO}_3^-] + [\text{CO}_3^{2-}], \quad (2.3)$$

and c is the concentration of CO_3^{2-} , which are expressed in units of $\mu\text{mol} \cdot \text{kg}^{-1}$. The strength of external CO_2 injection is ν and is of our main interest in this study. Time t is nondimensionalized by dividing the homeostat's dominant characteristic timescale τ_w which is about 10^5 years. Function $\bar{s} = 1 - s$. s is a sigmoidal function, and f is the ‘‘buffer function’’ as follow

$$s(c, c_p) = \frac{c^\gamma}{c^\gamma + c_p^\gamma}, \quad f(c) = f_0 \frac{c^\beta}{c^\beta + c_f^\beta}. \quad (2.4)$$

The parameter μ is a characteristic concentration, b is the maximum CaCO_3 burial rate, θ is the maximum respiration feedback rate, and ν is the CO_2 injection rate. The parameter c_x is the crossover CO_3^{2-} (respiration), c_p is the crossover CO_3^{2-} (burial), c_f is the crossover CO_3^{2-} (buffering), f_0 is the maximum buffer factor, and γ, β are the sigmoid sharpness indexes. The parameters $\mu, b, \theta, c_p, c_x, c_f, w_0, \gamma$ and β are constants and are set to fit in properties of the modern ocean. The value of these parameters are listed in [17, SI Appendix, Table S1]. We only change the value of c_x and ν in this article.

System (2.1-2.2) behaves as a Hopf bifurcation when parameter c_x varies. For $c_x < 55.89 \mu\text{mol} \cdot \text{kg}^{-1}$, there is only one stable fixed point (c^*, w^*) of the system. For $55.89 \mu\text{mol} \cdot \text{kg}^{-1} < c_x < 62.61 \mu\text{mol} \cdot \text{kg}^{-1}$, a stable fixed point and a stable limit cycle appear and an unstable limit cycle lies in between as is shown in Figure 2. For $c_x > 62.61 \mu\text{mol} \cdot \text{kg}^{-1}$, there is a stable limit cycle and an unstable fixed point. For detailed analysis and explanation of the model, we refer readers to [17].

In the real world, there are unexpected events that would slightly change the carbon input rate ν . For example, the Anak Krakatau volcano erupted suddenly in April, 2020 and released massive carbon dioxide compared to a common volcanic eruption. But this amount of carbon dioxide is still very small compared to the total released carbon dioxide characterized by ν . The instrument error may also lead to disruption to the carbon input rate ν . So, we include a random perturbation to the parameter ν with sufficient small amplitude ϵ . This gives us the following stochastic system:

$$dc = [\mu[1 - bs(c, c_p) - \theta\bar{s}(c, c_x) - \nu] + w - w_0] f(c) dt - \epsilon \mu f(c) dB_t^1, \quad (2.5)$$

$$dw = [\mu[1 - bs(c, c_p) + \theta\bar{s}(c, c_x) + \nu] - w + w_0] dt + \epsilon \mu dB_t^2, \quad (2.6)$$

where B_t^1 and B_t^2 are two standard Brownian motions.

No matter how small the random perturbation is, the original stable state would become a metastable state. And after a sufficient long time, the solution to (2.5-2.6) would transport from one metastable state to another metastable state. That means, for the parameter c_x lying in the bistable regime ($55.89 \mu\text{mol} \cdot \text{kg}^{-1}, 62.61 \mu\text{mol} \cdot \text{kg}^{-1}$), the solution to system (2.5-2.6) will go from the stable state (c^*, w^*) to the oscillatory state, that is the stable limit cycle of the deterministic system (2.1-2.2).

We will focus on the bistable case, that is $55.89 \mu\text{mol} \cdot \text{kg}^{-1} < c_x < 62.61 \mu\text{mol} \cdot \text{kg}^{-1}$. In the next section, we will introduce a large deviation approach that enables us to capture this transition phenomena.

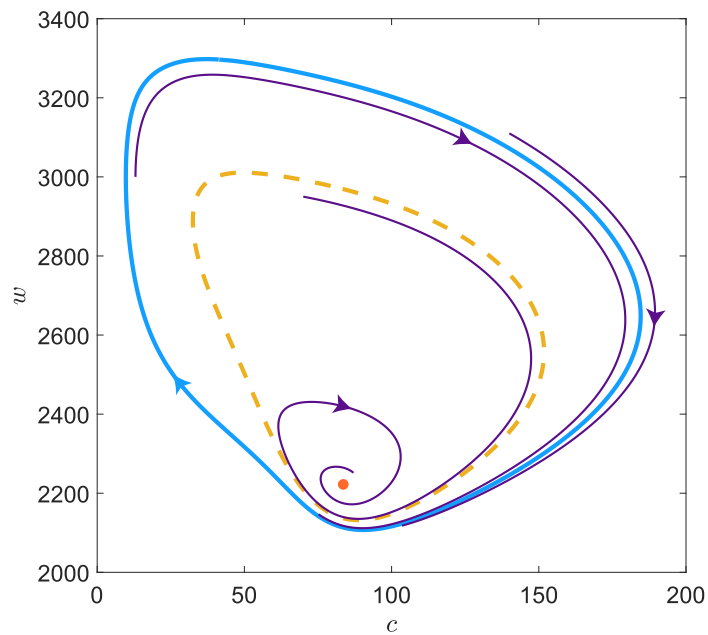


Figure 2: Phase-space trajectories in the bistable regime. Here $c_x = 57 \mu\text{mol} \cdot \text{kg}^{-1}$. The yellow dashed limit cycle is unstable. Trajectories (purple arrow lines) initialized inside the unstable limit cycle return to the stable fixed point (the reddish orange point). Trajectories (purple arrow lines) initialized outside the unstable limit cycle evolve to the stable limit cycle (the blue arrow loop).

3 A large deviation approach

We will briefly introduce the large deviations theory and the geometric minimum action method based on it.

We consider a generalized stochastic differential equation in \mathbb{R}^2 of equation (2.5-2.6) as follows,

$$dX^\epsilon(t) = \kappa(X^\epsilon(t))dt + \epsilon\eta(X^\epsilon(t))dB(t), \quad X^\epsilon(0) = x_0, \quad (3.1)$$

where $\kappa : \mathbb{R}^2 \rightarrow \mathbb{R}^2$ is a regular function, $\eta : \mathbb{R}^2 \rightarrow \mathbb{R}^{2 \times 2}$ is a 2×2 matrix-valued function and B is a standard Brownian motion in \mathbb{R}^2 .

Under some assumptions on the coefficients κ and η , for instance, the Lipschitz continuous conditions, the solution X^ϵ to equation (3.1) satisfies a large deviation principle with an action functional S_T . It enables us to estimate the probability that X^ϵ stays in a δ -neighborhood of a path ψ through the following asymptotic relation.

$$\mathbb{P}(d(X^\epsilon, \psi) < \delta) \sim \exp\left(-\frac{1}{\epsilon}S_T(\psi)\right), \quad \text{as } \epsilon \rightarrow 0, \quad (3.2)$$

where d is the distance in \mathbb{R}^2 . The action functional S_T is

$$S_T(\varphi) = \int_0^T L(\varphi, \dot{\varphi})dt, \quad (3.3)$$

with the Lagrange functional

$$L(\varphi, \dot{\varphi}) = \frac{1}{2}(\dot{\varphi} - \kappa(\varphi))(\eta\eta^T(\varphi))^{-1}[\dot{\varphi} - \kappa(\varphi)].$$

The large deviation theory also equips us to capture the long time behaviors of X^ϵ with quasi-potential V . That is

$$V(x_1, x_2) = \inf_{T>0} \inf_{\varphi \in \bar{C}_{x_1}^{x_2}(0,T)} S_T(\varphi), \quad (3.4)$$

where $\bar{C}_{x_1}^{x_2}(0, T)$ is the space of all absolutely continuous functions that start at x_1 and end at x_2 . Assume that there exists a path $\tilde{\varphi}$ and time $\tilde{T} \in [0, \infty]$ satisfying,

$$V(x_1, x_2) = S_{\tilde{T}}(\tilde{\varphi}).$$

Then, in probability 1, the sample paths of X^ϵ from x_1 to a δ -neighborhood of x_2 , converge to $\tilde{\varphi}$ when the noise intensity ϵ and the neighborhood size δ tend to 0 as well as the time T tends to \tilde{T} . This result means that the sample path $\tilde{\varphi}$ is the most probable transition path we are looking for. Readers may refer to [15, Proposition 2.3] for a more precise statement.

In summary, we only need to find the minimizer of equation (3.4) to obtain a most probable transition path between two metastable states. For a most probable transition path between a metastable state and an oscillatory state D , for example, a limit cycle, we need to find the minimizer of the following equation.

$$V(x, D) = \inf_{y \in D} V(x, y) = \inf_{y \in D} \inf_{T>0} \inf_{\varphi \in \bar{C}_x^y(0,T)} S_T(\varphi). \quad (3.5)$$

We will conduct a geometric minimum action method introduced in [15] to find the most probable transition path between the stable fixed point and points near the limit cycle. Then, we pick up the path which has the minimum quasi-potential as the most probable transition path between the stable state and the limit cycle. That is the minimizer to equation (3.5).

4 Numerical simulations and discussions

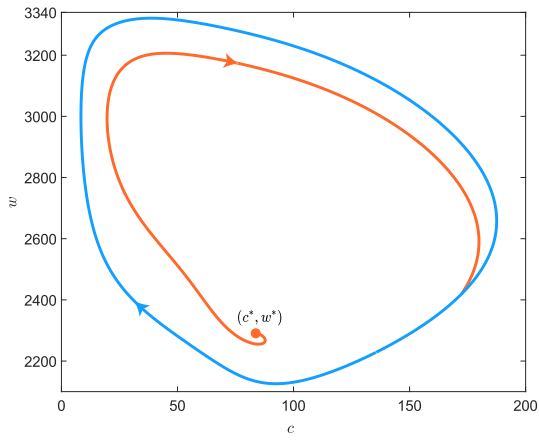
In this section, we will present the most probable transition paths that are computed through the geometric minimum action method. We are interested in how the most probable transition path changes as the external CO₂ input rate ν varies, in order to better understand this carbonate system.

We choose $c_x = 62$ and use the Euler scheme to simulate the limit cycle value, that is the oscillatory state of the carbonate system. We calculate the most probable transition path from the stable state (c^*, w^*) to a point near the oscillatory state, for ν from 0 to 0.9. 3000 points on the transition path are made to be equidistant. The quasi-potential between two points on the limit cycle is zero, because there is a deterministic orbit connecting each other though the limit cycle and this makes the action achieve its minimum 0. In practice, as we do not actually choose points on the limit cycle, we can obtain a most probable transition path though the geometric minimum action method. Then, we only need to find the path with the least quasi-potential as the most probable transition path connecting the stable state (c^*, w^*) and the oscillatory state. The most probable transition paths for $\nu = 0, 0.19, 0.2$ and 0.4 are shown in Figure 3 in the c - w plane.

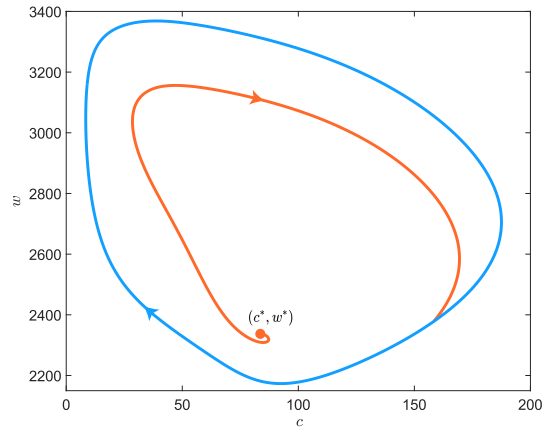
The most probable transition path has to travel a longer way to achieve the oscillatory state for $\nu < 0.2$ as is shown in Figure 4. The dramatic change happens near $\nu = 0.2$. The most probable transition path stops ending at the “southeast” part of the limit cycle and starts to end at the “southwest” part of the limit cycle as is shown in Figure 3. Consequently, the oscillatory ranges for c and w on the most probable transition path shrink. And the arrival value of concentration of CO₃²⁻ decreases from above 150 $\mu\text{mol} \cdot \text{kg}^{-1}$ to around 50 $\mu\text{mol} \cdot \text{kg}^{-1}$.

If we look into how c , the concentration of CO₃²⁻, changes with respect to time, we find two different patterns for transitions. Again, we use Euler scheme to generate the data of c before and after transition for noise strength $\epsilon = 0.01$. Then we connect them with the most probable transition path and illustrate the results in in Figure 4. When the the external CO₂ rate ν is smaller than a threshold near 0.2, the concentration of CO₃²⁻ will undergo an excursion, whose size is slightly smaller than the oscillatory state (the limit cycle shown in Figure 3, to shift to the oscillatory state. When ν exceeds the threshold near 0.2, the concentration of CO₃²⁻ will undergo a much smaller excursion to shift to the oscillatory state. This result implies that at more that 20% external carbon input rate, much less changes to the concentration of CO₃²⁻ may lead to a transition.

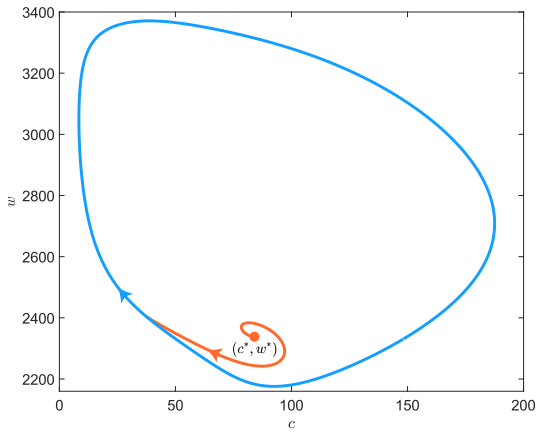
Our calculation shows the early warning sign of the carbonate system. If the solution (c, w) stays near the stable state (c^*, w^*) , the carbonate system of the ocean and the carbon cycle are in dynamic equilibrium. But when the solution (c, w) enters the oscillatory state (the stable limit cycle), the carbonate system of the ocean will change dramatically and may cause massive extinction [17]. It is important to identify the transition between these two



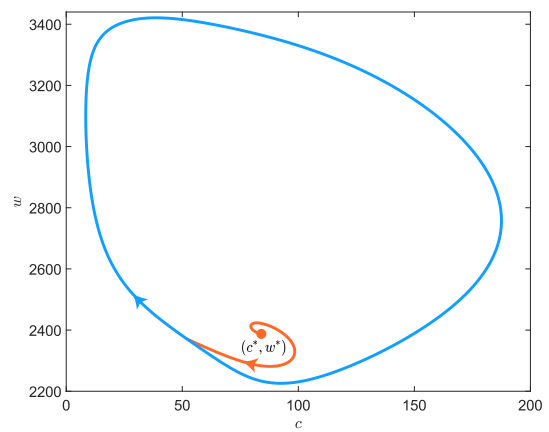
(a) $\nu = 0$



(b) $\nu = 0.19$

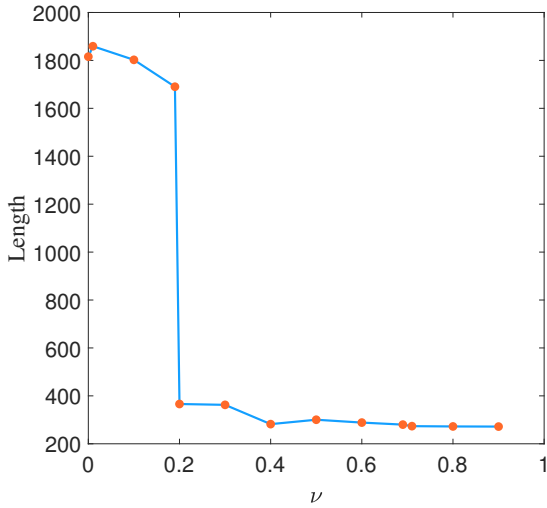


(c) $\nu = 0.2$

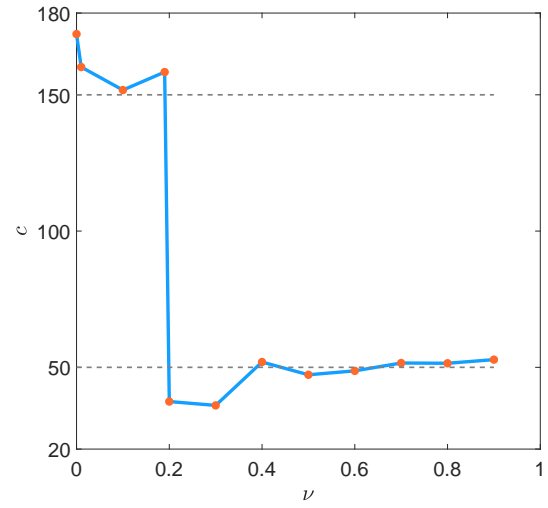


(d) $\nu = 0.4$

Figure 3: Most probable transition paths (reddish orange arrow lines) from the metastable state (c^*, w^*) (orange point) to the oscillatory state (blue limit cycle) for external CO_2 input rate $\nu = 0, 0.19, 0.20, 0.4$ and parameter $c_x = 62$.

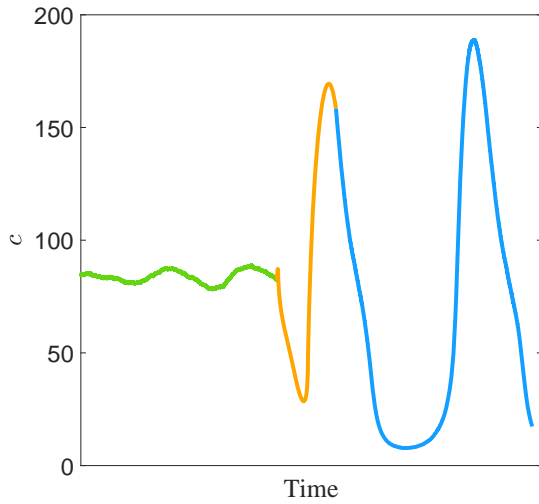


(a) The length for the most probable transition path

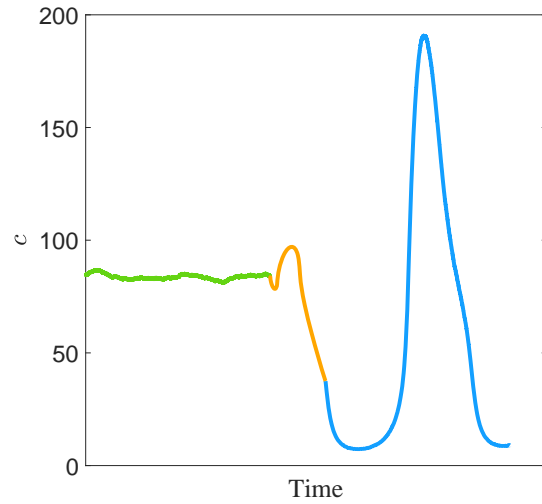


(b) The arrival value of c

Figure 4: The length for the most probable transition path and the arrival value of concentration of CO_3^{2-} , c , with respect to different external CO_2 input rate ν . Parameter $c_x = 62$. Critical changes happen around $\nu = 0.2$. The length of most probable transition path decreases to lower than 400. The arrival value of c decreases from $150 \mu\text{mol} \cdot \text{kg}^{-1}$ to around $50 \mu\text{mol} \cdot \text{kg}^{-1}$.



(a) Transition in view of c for $\nu = 0.19$



(b) Transition in view of c for $\nu = 0.2$

Figure 5: Illustrations for transitions in view of c , the concentration of CO_3^{2-} , for CO_2 input rate $\nu = 0.19, 0.2$ and parameter $c_x = 62$. The orange line is the value of c on the most probable transition path. The green line represents the value of c near the metastable state and the blue line represents the value of c on the oscillatory state.

states. Our calculation shows two transition patterns of c , the concentration of CO_3^{2-} (See Figure 5): (i) At a lower level external CO_2 input rate (lower than 20%), c will first drop to lower than $50 \mu\text{mol} \cdot \text{kg}^{-1}$ and then increase to higher than $150 \mu\text{mol} \cdot \text{kg}^{-1}$, before transferring to the oscillatory state. (ii) But at a higher level external CO_2 input rate (larger than 20%), c will only increase a little to around $100 \mu\text{mol} \cdot \text{kg}^{-1}$ and then drop to around $50 \mu\text{mol} \cdot \text{kg}^{-1}$ to enter the oscillatory state. Given the external CO_2 input rate, we can identify the transition before the system enters the oscillatory state.

In conclusion, we have computed the most probable transition path connecting a metastable state and an oscillatory state for a carbonate system under random fluctuations in the external CO_2 input rate. As the external CO_2 input rate ν changes, two different transition patterns occur with $\nu \approx 0.2$ as a critical value (See Figure 5): (i) At a lower level external CO_2 input rate (lower than 20%), the concentration of CO_3^{2-} undergoes a larger excursion to shift to the oscillatory state. (ii) But at a higher level external CO_2 input rate (larger than 20%), a much smaller excursion of the concentration of CO_3^{2-} leads to a transition to the oscillatory state. Moreover, as the external CO_2 input rate ν increases, the arrival value of the concentration of CO_3^{2-} decreases from over $150 \mu\text{mol} \cdot \text{kg}^{-1}$ to around $50 \mu\text{mol} \cdot \text{kg}^{-1}$. (Figure 4b).

Acknowledgements

This work was partly supported by the NSFC grants 11771449.

Data Availability

The data that support the findings of this study are openly available in GitHub.
<https://github.com/JayWeiss/CarbonCycle-gMAM>

References

- [1] L. Arnold. *Random Dynamical Systems*. Springer, Berlin, 2003.
- [2] J. L. Creaser, K. Tsaneva-Atanasova, and P. Ashwin. Sequential noise-induced escapes for oscillatory network dynamics. *SIAM Journal on Applied Dynamical Systems*, 17:500–525, 2018.
- [3] R. de la Cruz, R. Perez-Carrasco, P. Guerrero, T. Alarcon, and K. M. Page. Minimum action path theory reveals the details of stochastic transitions out of oscillatory states. *Physical Review Letters*, 120:128102, Mar 2018.
- [4] P. D. Ditlevsen. Observation of α -stable noise induced millennial climate changes from an ice-core record. *Geophysical Research Letters*, 26(10):1441–1444, 1999.
- [5] J. Duan. *An Introduction to Stochastic Dynamics*. Cambridge University Press, 2015.

- [6] J. Duan and W. Wei. *Effective Dynamics of Stochastic Partial Differential Equations*. Elsevier, 2014.
- [7] P. Imkeller and J.-S. Von Storch. *Stochastic Climate Models*, volume 49. Birkhäuser, 2012.
- [8] Y. Li, R. Mei, Y. Xu, J. Kurths, J. Duan, and R. Metzler. Particle dynamics and transport enhancement in a confined channel with position-dependent diffusivity. *New Journal of Physics*, 22(5):053016, 2020.
- [9] Y. Li, Y. Xu, and J. Kurths. First-passage-time distribution in a moving parabolic potential with spatial roughness. *Physical Review E*, 99(5):052203, 2019.
- [10] Y. Li, Y. Xu, J. Kurths, and J. Duan. The influences of correlated spatially random perturbations on first passage time in a linear-cubic potential. *Chaos: An Interdisciplinary Journal of Nonlinear Science*, 29(10):101102, 2019.
- [11] Y. Li, Y. Xu, J. Kurths, and X. Yue. Lévy-noise-induced transport in a rough triple-well potential. *Physical Review E*, 94(4):042222, 2016.
- [12] L. Lin, H. Yu, and X. Zhou. Quasi-potential calculation and minimum action method for limit cycle. *Journal of Nonlinear Science*, 29:961–991, 2019.
- [13] J. Ma, Y. Xu, Y. Li, R. Tian, G. Chen, and J. Kurths. Precursor criteria for noise-induced critical transitions in multi-stable systems. *Nonlinear Dynamics*, 101(1):21–35, 2020.
- [14] J. Ma, Y. Xu, Y. Li, R. Tian, and J. Kurths. Predicting noise-induced critical transitions in bistable systems. *Chaos: An Interdisciplinary Journal of Nonlinear Science*, 29(8):081102, 2019.
- [15] M. Heymann and E. Vanden-Eijnden. The geometric minimum action method: A least action principle on the space of curves. *Communications on Pure and Applied Mathematics*, LXI:1052–1117, 2008.
- [16] B. Qiu and W. Miao. Kuroshio path variations south of Japan: Bimodality as a self-sustained internal oscillation. *Journal of Physical Oceanography*, 30(8):2124–2137, 2000.
- [17] D. H. Rothman. Characteristic disruptions of an excitable carbon cycle. *Proceedings of the National Academy of Sciences*, 116(30):14813–14822, 2019.
- [18] Z. Wang, Y. Xu, and H. Yang. Lévy noise induced stochastic resonance in an fhm model. *Science China Technological Sciences*, 59(3):371–375, 2016.